Cancer Chemother Pharmacol (1995) 35: 403–410

ORIGINAL ARTICLE

Mary E. Fox · Paul J. Smith

Subcellular localisation of the antitumour drug mitoxantrone and the induction of DNA damage in resistant and sensitive human colon carcinoma cells

Received: 9 May 1994 / Accepted: 16 August 1994

Abstract Cellular uptake and subcellular localisation of the antitumour agent mitoxantrone were studied in a human colon-carcinoma cell line and a mitoxantrone-resistant subline showing features consistent with an atypical multidrug-resistance phenotype involving altered topoisomerase II. Flow cytometry indicated a reduced uptake of mitoxantrone in the resistant line. Confocal microscopy indicated that mitoxantrone-associated fluorescence was primarily found within discrete cytoplasmic inclusions and around the periphery of the nucleus, with low levels being observed within the nucleus. The frequency of cytoplasmic inclusions was reduced in mitoxantrone-resistant cells as compared with parental cells. Fluorescence in cytoplasmic inclusions persisted throughout a 24-h post-treatment period in both cell lines. The results suggest that the persistence of mitoxantrone in cells is a determinant for the continuous induction of DNA damage, perhaps through chronic topoisomerase II trapping, and that modified sequestration may contribute to clinically relevant moderate levels of non-classic multidrug resistance.

Key words Mitoxantrone · Confocal microscopy
Drug resistance

Introduction

The anthraquinone mitoxantrone is an anticancer agent used in the treatment of acute leukaemia [13] and breast cancer [31]. The cytotoxic action of mitoxantrone is thought to relate to its ability to trap the nuclear enzyme DNA topoisomerase II as DNA-protein complexes (reviewed in [22]). Mitoxantrone is significantly more toxic towards human cells than are other antitumour DNA-intercalating topoisomerase II poisons such as amsacrine (mAMSA) and doxorubicin [12, 14, 33]. Several features of mitoxantrone may contribute towards the high cytotoxicity, including the intracellular persistence of mitoxantrone [8, 26], the unusual persistence of mitoxantrone-induced DNA damage [14, 16] and the mode of binding of drug molecules to DNA involving both electrostatic binding and intercalation [4, 18, 23].

Conventional fluorescence microscopy, flow cytometry [10, 19, 36] and confocal imaging [15, 35] have been used to measure the cellular uptake and subcellular distribution of naturally highly fluorescent drugs such as anthracyclines. However, mitoxantrone in solution has been found to demonstrate pH-dependent, extremely weak fluorescence, whereas the mitoxantrone diacid metabolite is essentially non-fluorescent [3]. We have previously reported [30] that intact mitoxantrone-treated human and murine cells exhibit low levels of fluorescence that are detectable by flow cytometry and confocal imaging, providing an opportunity to measure intracellular mitoxantrone deposition directly. In both methodologies, laser light excitation and high-gain photomultiplier fluorescence detection systems are employed. It is possible that the fluorescent species detected in mitoxantrone-treated cells may be a product of singlet-singlet transitions by free mitoxantrone or mitoxantrone-macromolecular charge-transfer complexes detected only under the intense laser light. Under such conditions the quantum yield of fluorescence from either free mitoxantrone or a charge-transfer complex may be increased to more readily detectable levels.

The objective of the present study was to use the complementary methods of flow cytometry and confocal microscopy to analyse changes in whole-cell and subcellular fluorescence patterns in living cells during and after mitoxantrone exposure and to relate this to the DNA-damaging characteristics of the drug in mitoxantrone-sensitive and -resistant human adenocarcinoma cells.

Mary E. Fox[1] · Paul J. Smith (✉)
MRC Clinical Oncology and Radiotherapeutics Unit, MRC Centre, Hills Road, Cambridge, CB2 2QH, UK

Present address:
[1] Department of Radiation Oncology, Division of Radiation Biology, Stanford University School of Medicine, Stanford, CA 94305, USA

Materials and methods

Cell lines, clonogenic assay and drugs

The human adenocarcinoma cell line WiDr/S2 is a subline derived in our laboratory from the WiDr/S line [25]. Likewise, WiDr/R3 is our subline of the mitoxantrone-resistant WiDr/R cell line. WiDr/R was originally obtained by continuous culture of WiDr/S cells in the presence of mitoxantrone ([33]; kindly provided by Dr. R. Wallace). Monolayer cultures were maintained in Eagle's minimal essential medium (Gibco) supplemented with 10% foetal calf serum, 100 IU penicillin/ml, 100 mg streptomycin/ml and 2 mM glutamine. Cultures were incubated at 37 °C in an atmosphere of 5% CO_2 in air and were routinely detached using trypsin ethylenediaminetetraacetic acid (EDTA). Clonogenicity was determined as described previously [14], and D_0 values (the dose required to reduce the surviving fraction by e^{-1}; a dose D_0 would give an average of one lethal event per member of a treated population) for exponential-form survival curves were obtained by computer analysis of the data [29]. Mitoxantrone (mitozantrone; Novantrone; kindly supplied by Lederle Laboratories) was stored as a 2 m*M* aqueous stock at −20 °C. Other drugs used were doxorubicin (Adriamycin; Farmitalia Carlo Erba), colcemid (Sigma), vincristine (David Bull Laboratories), camptothecin (Sigma), colchicine (Gibco), etopside (VP-16-Bristol-Myers) and mAMSA (amsacrine; Parke-Davis).

Filter-binding assay for DNA-protein cross-linking

The ability of crude nuclear 0.35 *M* salt protein extracts to bind to plasmid DNA in the presence of drugs was determined using the method described previously [24]. Briefly, reaction mixtures of 15 ng [^{35}S]-labeled pBR322 DNA, 1.0 μg nuclear protein extract, and mitoxantrone were filtered through polyvinyl chloride filters (2-μm pore size; Millipore) and the amount of DNA retained on the filter as DNA-protein complexes was determined by scintillometry.

K-sodium dodecyl sulphate precipitation of DNA-protein complexes

DNA-protein complexes were measured by an adaptation [1] of a method described previously [27]. Cells were plated in 24-well plates at a density of 8×10^4 cells/well and allowed to attach for 24 h. DNA was labeled with 0.05 μCi [^{14}C]-thymidine for 48 h, followed by a 2 to 4-h chase period in fresh medium. After 1 h exposure to drug, cells were washed twice with 0.02% EDTA in phosphate-buffered saline (PBS) and frozen on dry ice. The frozen cells were thawed slowly in an isotonic salt solution (8.0 g NaCl, 0.4 g glucose, 0.35 g $NaHCO_3$, 0.372 g EDTA per litre) and aliquots containing 1×10^5 cells were transferred to 2-ml Eppendorf tubes. Following centrifugation at 1,500 g in a Jouan MR 14.11 benchtop centrifuge, cell pellets were lysed by the addition of 1.2 ml lysis solution [1.0% sodium dodecyl sulphate (SDS), 5 m*M* EDTA, 0.4 mg calf thymus DNA/ml], vortexed and incubated at 65 °C for 10 min. Aliquots (200 μl) aliquots were removed for the determination of total radioactivity in each sample. DNA-protein complexes were precipated by the addition of 250 μl 650 m*M* KCl to the remaining lysate, vortexed for 30 s and incubated for 30 min on ice. The precipitates were washed three times by repeated centrifugation at 10,000 g, and the pellet was resuspended in 1 ml pre-warmed wash solution (10 m*M* TRIS-Cl, pH 8.0, 200 m*M* KCl, 1 m*M* EDTA, 0.1 mg calf thymus DNA/ml), vortexed for 30 s and incubated first at 65 °C for 10 min and then on ice for 10 min. The final pellet was re-suspended in 1 ml PBS, vortexed and incubated at 65 °C for 10 min prior to determination of radioactivity by liquid scintillometry and calculation of the percentage of the total counts precipitated.

Measurement of DNA strand breaks

Lesions detectable as DNA breaks under alkaline conditions, including protein-associated strand breaks, were measured by microscale adaptation [28] of the method described by Kanter and Schwartz [17]. Briefly, treated cells in microplate wells were subjected to: no denaturation (T), controlled alkali denaturation for 30 min (P), or complete denaturation (B; the same as for P but with sonication). DNA-specific fluorescence in each well was measured using a Fluoroskan II micro-plate fluorimeter (Flow Laboratories) with excitation at 355 nm and emission measured at 480 nm, and the percentage of double-stranded DNA (D) for each treatment was calculated as $D = 100(P-B)/(T-B)$. Drug-induced enhancement of DNA unwinding (F) was calculated by the equation $F = -100\log(Dx/Dc)$, where Dx and Dc represent the percentage of double-stranded DNA detected in treated and control samples, respectively.

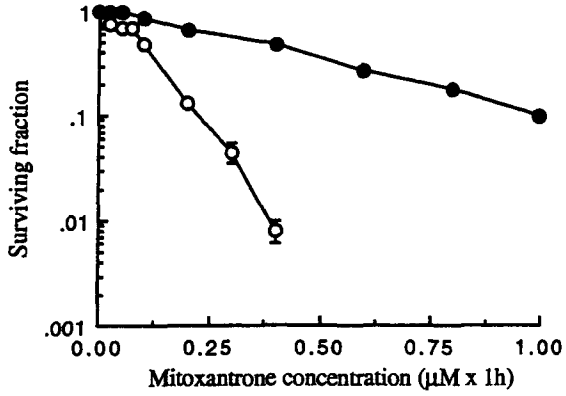

Fig. 1 Sensitivity of the human adenocarcinoma cell lines WiDr/S2 (○) and WiDr/R3 (●) to 1 h treatment with mitoxantrone. Cytotoxicity was assayed by measurement of the clonogenic potential of drug-treated cells. Points represent arithmetic means of 12 determinations; bars represent standard errors

Flow cytometry

Following 1 h exposure to mitoxantrone, cells were detached and resuspended in medium at a concentration of $1-2 \times 10^5$ cells/ml. Intracellular fluorescence was measured flow cytometrically using a system incorporating an argon laser tuned to a wavelength of 488 nm. Cell debris was excluded by gating on 90 ° light-scatter signals. Fluorescence emission at 630 nm was measured for a total of 1×10^4 cells for each sample.

Confocal microscopy

The method has been described elsewhere [30]. The system used was a Bio-Rad MRC-600 laser scanning confocal microscope employing a GHS filter block allowing excitation at 514 nm and the detection of red fluorescence. Cells were grown on sterile coverslips in 6-well plates for 48–72 h. Drug-treated coverslips were washed, mounted and observed using a x60 oil-immersion objective lens. Images were Kalman-filtered and analysed using the standard SOM software package (Bio-Rad Microsciences).

Results

Drug-resistance patterns

Initial studies confirmed the enhanced resistance of WiDr/R3 subline cells (Fig. 1; IC_{50} values of 0.1 and 0.4 μ*M* mitoxantrone for WiDr/S2 and WiDr/R3 cells, respectively [33]). Computer analysis of the survival data gave D_0 values

Table 1 Relative resistance of a drug-resistant human adenocarcinoma cell line to cytotoxic drugs. Mean data derived from 4 determinations for each drug (*RF* resistance factor)

Drug	Drug sensitivity (D_0 ; μM × 1 h) for cell line:		
	WiDr/S2	WiDr/R3	RF[a]
Mitoxantrone	0.08	0.38	4.8
Doxorubicin	1.9	2.7	1.4
VP-16	19.7	76.6	3.9
mAMSA	4.1	5.8	1.4
Camptothecin	1.9	2.0	1.1
Colchicine	4.1	2.8	0.69
Vincristine	1.6	1.8	1.1

[a] D_0 (resistant line)/D_0 (sensitive line)

of 0.08 μ*M* for WiDr/S2 and 0.38 μ*M* for WiDr/R3, representing ~5-fold resistance of WiDr/R3 to mitoxantrone relative to the parental line. The original mitoxantrone-resistant line WiDr/R was partially resistant to many, but not all, DNA-intercalating agents, including doxorubicin, daunorubicin, mAMSA and ellipticine, but retained sensitivity to mitotic spindle inhibitors [33]. In the present study the WiDr/R3 cell line displayed (Table 1) cross-resistance to VP-16 and marginal resistance to doxorubicin and mAMSA but remained sensitive to the topoisomerase I inhibitor camptothecin and the mitotic spindle inhibitors colchicine and vincristine as compared with WiDr/S2 cells. This pattern of cross-resistance is suggestive of a moderate 'atypical' multidrug resistance (at-MDR) phenotype [9]. In addition, immunocytochemistry techniques showed no staining of WiDr/S2 or WiDr/R3 cells using three separate monoclonal antibodies raised against P-glycoprotein, over-expression of which is associated with classic MDR [11].

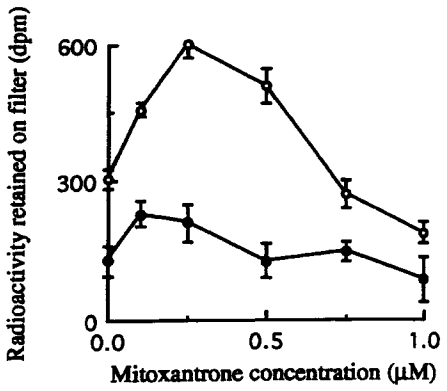

Fig. 2 Mitoxantrone-dependent DNA-protein cross-linking activities in 0.35 *M* NaCl nuclear extracts from sensitive WiDr/S2 (○) and resistant WiDr/R3 (●) cell lines. Data are mean values (± SE) for >3 determinations

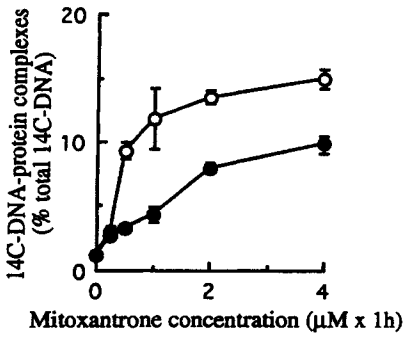

Fig. 3 Nuclear DNA-protein cross-linking measured as a percentage of total DNA precipitated in KCl/SDS at the end of 1 h exposure to mitoxantrone for WiDr/S2 (○) and WiDr/R3 (●) cells. Data are mean values (± SE) for 8 determinations

Drug-induced DNA-protein cross-linking in nuclear protein extracts

Comparison of the mitoxantrone-induced cross-linking activity of crude nuclear extracts revealed a dose-dependent DNA-protein cross-linking for both WiDr/S2 and WiDr/R3 (Fig 2), with maximal levels of cross-linking observed in the resistant cell line being more than 2-fold lower than those seen in the parental line. The analysis also indicated a reduced background level of cross-linking in WiDr/R3 cell extracts. This is consistent with a reduced availability or increased lability of type II topoisomerase enzyme in WiDr/R3 cells. Indeed, for equivalent total protein concentrations, the in vitro kinetoplast-DNA decatenation activity of crude nuclear extracts from the resistant cell line was consistently lower (~0.7-fold) than the activity of extracts of WiDr/S2 cells (data not shown).

Induction and persistence of DNA-protein complexes

The ability of mitoxantrone to trap topoisomerase II in intact WiDr/S2 and WiDr/R3 cells was determined by the indirect KCl/SDS precipitation technique. The induction of DNA-protein complexes by a 1-h exposure to mitoxantrone was found to be dose-dependent for both WiDr/S2 and WiDr/R3 cell lines (Fig. 3), the resistant line requiring a 4-fold greater concentration of mitoxantrone than the parental line to achieve protein cross-linking of 10% of the total DNA. Background corrected values for DNA-protein cross-linking induced by 1 μ*M* mitoxantrone were 10.6% ± 2.3% and 3.3% ± 0.6% after 1 h drug treatment and 7.9% ± 0.3% and 2.6% ± 0.2% after 4 h incubation in drug-free medium for WiDr/S2 and WiDr/R3 cell lines, respectively. Thus, there was persistence of >75% of the mitoxantrone-induced complexes in both cell lines.

Induction and persistence of DNA strand breaks induced by mitoxantrone

Analysis of the enhancement of DNA unwinding under alkaline conditions provides a method for detecting increases in total strand break frequencies, including those arising from DNA topoisomerase II trapping. Acute exposure to mitoxantrone was found to induce DNA strand breakage in both WiDr/S2 and WiDr/R3 cells in a dose-dependent manner (Fig 4), with lower levels of breakage

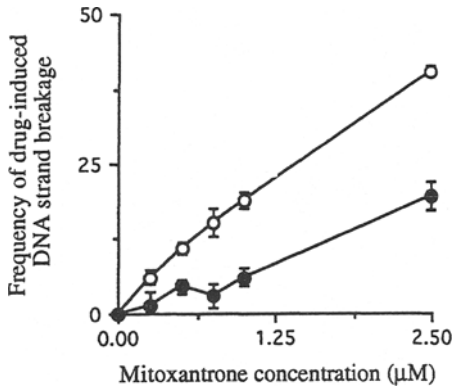

Fig. 4 Induction of nuclear DNA strand cleavage as detected after alkali treatment following acute exposure (1 h) of WiDr/S2 (○) and WiDr/R3 (●) cells to mitoxantrone. Values are the means (± SE) of 12–16 determinations

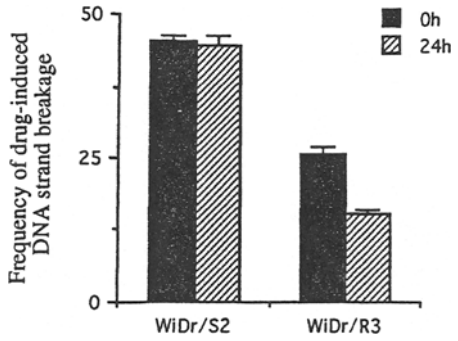

Fig. 5 Generation and disappearance of mitoxantrone-induced nuclear DNA strand cleavage as detected after alkali treatment. DNA strand breakage was assayed at the end of 1 h exposure to 1 μ*M* mitoxantrone (*filled columns*) and after 24 h post-treatment incubation in drug-free medium (*hatched columns*). Values are the means (± SE) of 12–16 determinations

occurring in the resistant line at all drug concentrations. The data support a correlation between the induction of DNA-protein complexes and DNA strand breaks. Initial levels of strand breaks induced by 1 μ*M* mitoxantrone were estimated to be ~2.9 breaks/10^9 Da DNA for WiDr/S2 cells and ~1 break/10^9 Da DNA for WiDr/R3 cells by reference to X-irradiated cells (data not shown). At the end of a 24-h post-treatment period in drug-free medium, DNA strand breaks persisted at the initial level in the parental line, whereas there was a ~40% reduction ($P < 0.0001$; Student's *t*-test) in the level detected in the resistant line (Fig. 5).

Measurement of mitoxantrone uptake by flow cytometry

WiDr/R3 cells consistently showed up to 35% lower initial levels of mitoxantrone-associated fluorescence than did WiDr/S2 cells (Fig. 6), consistent with the findings of Wallace et al. [33] that indicated a reduced level of radiolabeled drug uptake in resistant cells. The median fluorescence intensity of WiDr/S2 cells at 24 h after removal of drug was similar to that measured at the end of

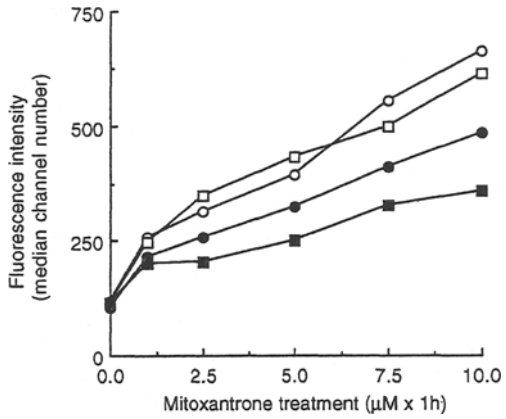

Fig. 6 Flow cytometric analysis of the initial uptake and retention of mitoxantrone by WiDr/S2 (*open symbols*) and WiDr/R3 (*filled symbols*) cells. Fluoresence at 630 nm was measured at the end of 1 h drug treament (*circles*) and following 24 h post-treatment incubation in drug-free medium (*squares*)

drug treatment. The median fluorescence intensity of WiDr/R3 cells at 24 h was consistently lower than the level measured at the end of drug treatment, suggesting that the degree of retention of mitoxantrone in the resistant line is lower than that in the sensitive parental line.

Subcellular distribution of mitoxantrone determined by confocal microscopy

Analysis of intracellular fluorescence following 1 h exposure of WiDr/S2 and WiDr/R3 cells to increasing concentrations of mitoxantrone revealed a drug dose-dependent increase in fluorescence for both cell lines (Fig. 7). In both cell lines, fluorescence was initially seen as bright punctate regions in the cytoplasm, presumed to reflect sequestration of mitoxantrone in cytoplasmic inclusions. At concentrations of 5 μ*M* and above, mitoxantrone accumulated mainly around the periphery of the nucleus and in intranuclear structures assumed to be nucleoli on the basis of their size, position and form. At all mitoxantrone concentrations studied the degree of nuclear fluorescence was low, with most of the fluorescence being perinuclear or nuclear membrane-associated. Pre-treatment with colcemid to increase the mitotic index revealed that mitotic chromosomes (indicated by arrows) were fluorescently stained (Fig. 7e, j). The significance of this observation is not clear but may reflect either the more compact nature of the DNA in condensed chromosomes or the enhanced access of mitoxantrone to chromatin upon breakdown of the nuclear membrane.

An attempt to quantify the distribution of mitoxantrone in WiDr/S2 and WiDr/R3 cells was made using an image-analysis approach. A mitoxantrone concentration of 5 μ*M* was chosen for this analysis since this appeared to be a non-saturating dose for both cell lines. For microcolonies covering equivalent areas (~13,000 μm^2) the fluorescence intensities were colour-coded such that the bright punctate

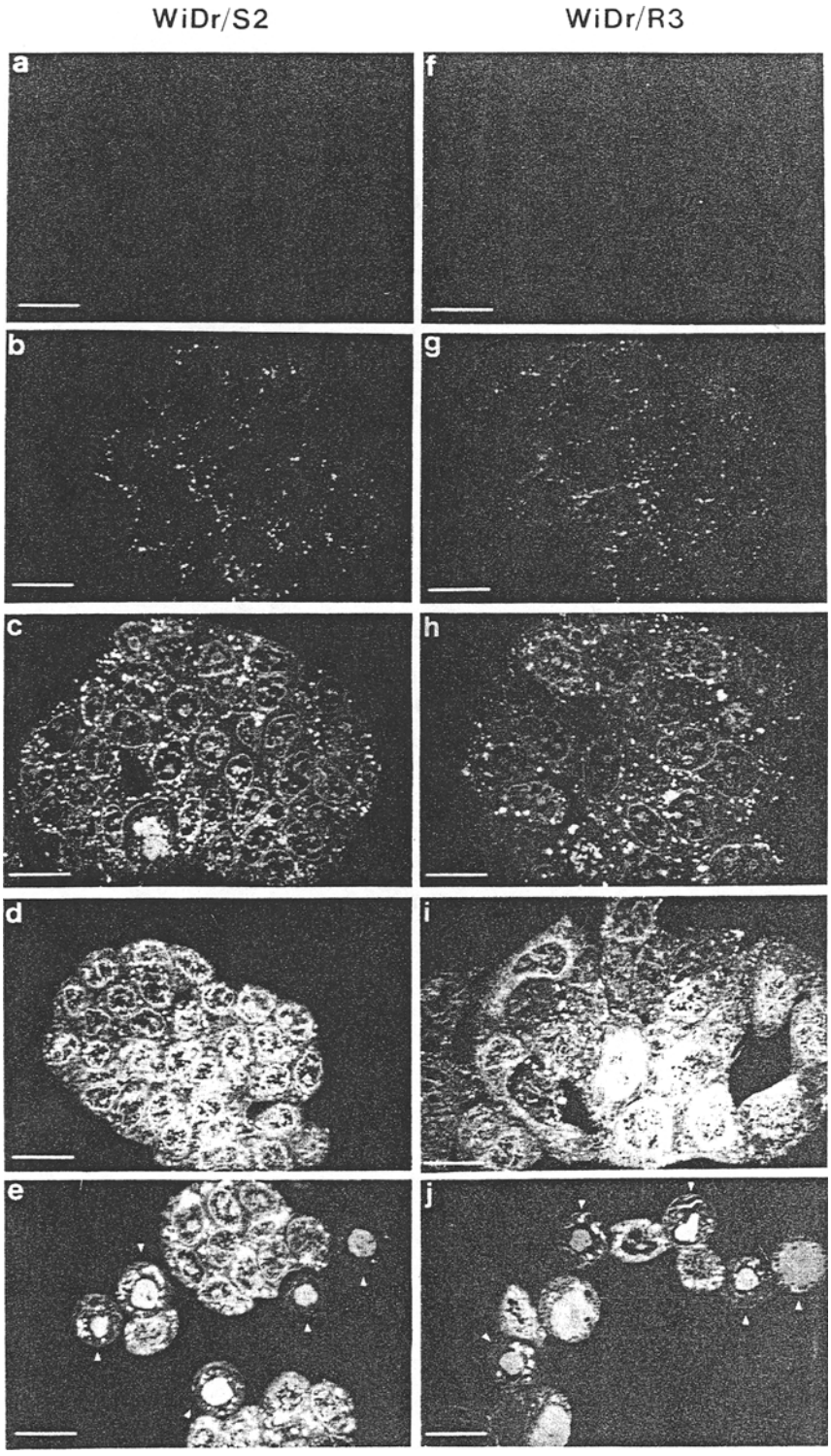

Fig. 7a–j Uptake and subcellular distribution of mitoxantrone in WiDr/S2 (**a–e**) and WiDr/R3 (**f–j**) cells as a function of drug concentration. Cells were viewed by confocal microscopy at the end of 1 h exposure to mitoxantrone. Bars = 25 μm. **a, f** Untreated cells. **b, g** 1 μ*M* mitoxantrone. **c, h** 5 μ*M* mitoxantrone. **d, i** 10 μ*M* mitoxantrone. **e, j** 10 μ*M* mitoxantrone following 12 h incubation in the presence of 60 ng colcemid/ml (mitotic cells are indicated by *arrows*)

fluorescence could be distinguished from the lower levels of background fluorescence. For each coded level of fluorescence, the fluorescence intensity per pixel and the total number of pixels were analysed, representative microcolonies being shown in Fig. 7 (c, h). Analysis of the fluorescence intensity per pixel revealed no difference in the fluorescence per unit area for either punctate or background fluorescence between the two cell lines. However, the total number of brightly fluorescent cytoplasmic locations in the area analysed was found to be 4 times greater in WiDr/S2 cells than in the resistant WiDr/R3 cells.

Subcellular distribution and retention of mitoxantrone

Following exposure to 5 μ*M* mitoxantrone, cells were either viewed immediately or washed and incubated in drug-free medium for a further 24 h prior to analysis. As noted above,

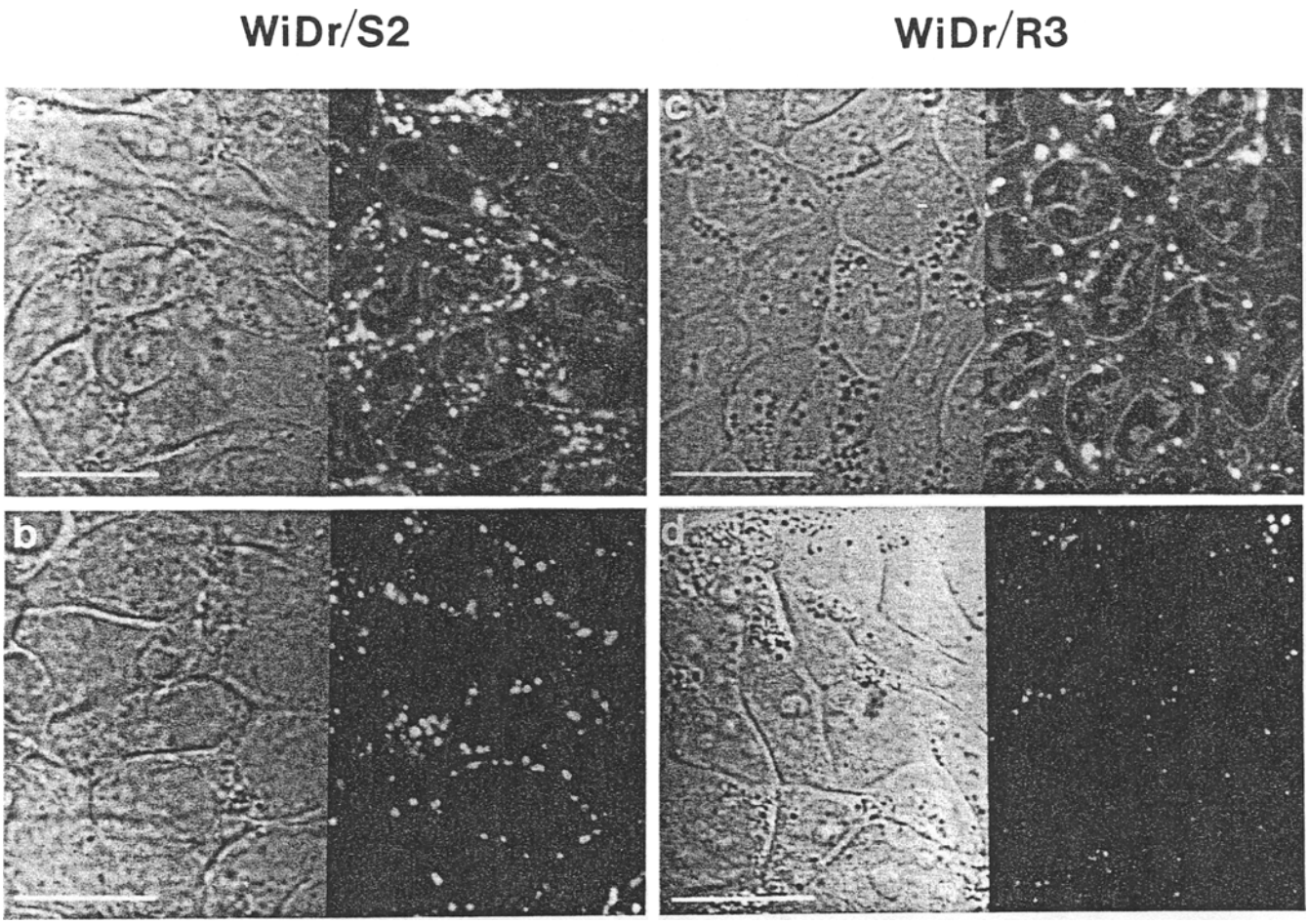

Fig. 8a–d Uptake and retention of mitoxantrone by WiDr/S2 (**a, b**) and WiDr/R3 (**c, d**) cells. Following 1 h exposure to 5 μ*M* mitoxantrone, cells either were viewed immediately (**a, c**) or were washed and incubated for 24 h in drug-free medium prior to viewing (**b, d**). The photographs show transmission (*left*) and fluorescence (*right*) images of representative microcolonies of cells for each treatment. Bars = 25 μm

at the end of acute drug treatment, mitoxantrone-associated fluorescence appeared predominantly within cytoplasmic inclusions and nucleoli-like structures and at nuclear membranes (Fig. 8), with fewer fluorescent cytoplasmic inclusions being present in the resistant cell line as compared with the sensitive cell line. Following 24 h post-treatment incubation, all of the low-level cytoplasmic and nuclear-associated fluorescence had disappeared. However, mitoxantrone-associated fluorescence persisted in the cytoplasmic inclusions in both cell lines, revealing the reduced frequency of such inclusions in the resistant cell line as compared with the sensitive line.

Discussion

The drug-sensitivity profile and DNA damage-induction characteristics of the WiDr/R3 cell line suggest the moderate expression of an at-MDR-like phenotype. The application of fluorometry to intact cells reveals the additional involvement of reduced cellular accumulation and modified subcellular distribution of mitoxantrone within discrete cytoplasmic compartments of WiDr/R3 cells. We suggest that reduced accumulation is associated with a reduced availability of intracellular structures capable of sequestering drug molecules. Mitoxantrone-induced DNA-protein cross-links were found to persist in both sensitive and resistant cells, suggesting that the longevity of the nuclear DNA-drug interaction was similar for both lines. Over a 24 h post-treatment period there was a complete loss of nuclear-located fluorescence in both cell lines, whereas there was a reduction in persistent DNA strand cleavage in the resistant line alone. Although nuclear-associated fluorescence is a monitor of intracellular drug delivery, its full interpretation is problematic and may represent the excitation of drug molecules not actively available for topoisomerase trapping. The study indicates that mitoxantrone is sequestered for long periods in cytoplasmic inclusions, and reduced availability of this compartment may be a component of multifactoral drug resistance.

Previous studies [3, 30] have established the basis for the fluorometric detection of mitoxantrone. In solution, the drug shows a spectrum with a low absorbance at 514 nm and maxima of equal peak heights at 610 and 660 nm [3]. The mitoxantrone fluorescence-emission spectrum for excitation at a 610-nm wavelength has a λ_{max} beyond the

visible range at 680–690 nm, with significant levels (>15% peak intensity) extending to wavelengths of ≥800 nm. The mitoxantrone diacid metabolite is essentially non-fluorescent [3]. DNA has a quenching effect on mitoxantrone fluorescence that becomes saturated (<50% decrease) at high DNA:drug molar ratios. Quenching is far less pronounced at emission wavelengths of >700 nm. In parallel confocal microscopy studies (P. J. Smith, unpublished data) we have used a range of excitation wavelengths (488, 514 and 647 nm) and monitored various fluorescence-emission wavelength regions (>520, >550 and >680 nm, respectively). Such spectral analyses confirmed that the general patterns for intracellular fluorescence were similar for the different excitation/emission wavelengths studied. These preliminary results suggest that fluorescence quenching is not a dominant factor in the overall low levels of intranuclear fluorescence and suggest a protective effect of an intact nuclear membrane on drug-DNA interactions.

The question arises as to the significance of the nuclear fluorescence signals monitored. The granular fluorescence observed in nuclei of mitoxantrone-treated cells may be enhanced by some loss of fluorescence upon binding of drug to DNA [3] and the persistent fluorescence upon binding to other subnuclear components. Consequently, the relatively homogeneous fluorescent staining of mitotic nuclei described herein, and of chromosome spread preparations (P. J. Smith, unpublished observations) may reflect the highly compact nature of the nuclear material rather than any change in drug binding/fluorescence per se. Under such circumstances, persistent binding of mitoxantrone to DNA in cells incubated in drug-free medium may not be detectable by fluorometry, explaining the persistence of drug-induced damage in WiDR/S2 cells. Interestingly, although overall nuclear fluorescence was low at all mitoxantrone concentrations studied, staining of nuclear components resembling nucleoli was observed in both cell lines at doses above 5 μ*M*, consistent with the preferential binding of mitoxantrone to nucleolar DNA and condensation of ribopolymers [5, 18].

The use of simple image-analysis methods to quantify the amount of fluorescence in different subcellular compartments indicated that WiDr/R3 cells showed a reduction in the total number of cytoplasmic inclusions sequestering drug. The identity of the cytoplasmic inclusions containing high concentrations of mitoxantrone described herein is not clear. There is evidence that drugs may be accumulated by mitochondria [20] and by lysosomes [21]. Preliminary experiments using the vital mitochondrion-staining dye rhodamine 123 indicated that mitochondria did not co-localise with the areas of mitoxantrone accumulation (results not shown). However, the possible role of lysosomes in the cytoplasmic sequestration and metabolic activation of mitoxantrone merits further investigation. Although mitoxantrone may initiate its cytotoxic actions primarily through the induction of DNA damage [6, 16, 29, 32], reduced cytoplasmic accumulation of drug may be an important secondary factor and effect moderate levels of resistance. Indeed, drug-localisation studies with anthracyclines and *Vinca* alkaloids have suggested differences between sensitive and resistant cell lines in the relative sizes of fast- and slow-releasing pools [2, 36].

Mitoxantrone sequestered in the cytoplasm was found to persist in both WiDr/S2 and WiDr/R3 cell lines over a 24-h post-treatment period. The continued retention of mitoxantrone in sensitive cell lines has been noted previously [8, 26] together with a possible binding to cytokeratins [7]. If the free concentration of drug in cells is low, the slow release of mitoxantrone from these cytoplasmic inclusions and its subsequent availability to nuclear DNA and topoisomerase II may explain the unusually persistent DNA cleavage [14]. The results presented herein suggest that the degree of sequestration and cytoplasmic retention of mitoxantrone could be important factors determining cytotoxicity.

Acknowledgements The authors are grateful to the Dr Hadwen Trust for Humane Research for the provision of funds to purchase the microplate fluorometer and to Dr. J. V. Watson for the use of the flow cytometry facility.

References

1. Arundel CA, Vines CM, Tofilon PJ (1988) Chromatin modifications associated with *N*-methylamide-induced radiosensitization of clone A cells. Cancer Res 48: 5669
2. Beck WT, Cirtain MC, Lefko JL (1983) Energy-dependent reduced drug binding as a mechanism of *Vinca* alkaloid resistance in human leukaemic lymphoblasts. Mol Pharmacol 24: 485
3. Bell DH (1988) Characterization of the fluorescence of the antitumour agent, mitoxantrone. Biochim Biophys Acta 949: 132
4. Bowden GT, Roberts R, Alberts DS, Peng Y-M, Garcia D (1985) Comparative molecular pharmacology in leukaemic L1210 cells of the anthracene anticancer drugs mitoxantrone and bisantrene. Cancer Res 45: 4915
5. Chegini N, Safa AR (1987) Influence of mitoxantrone on nucleolar function in MDA-MB-231 human breast cancer cell line. Cancer Lett 37: 327
6. Crespi MD, Ivanier SE, Genovese J, Baldi A (1986) Mitoxantrone affects topoisomerase activities in human breast cancer cells. Biochem Biophys Res Commun 136: 521
7. Cress AE, Roberts RA, Bowden GT, Dalton WS (1988) Modification of keratin by the chemotherapeutic drug mitoxantrone. Biochem Pharmacol 37: 3043
8. Dalton WS, Cress AE, Alberts DS, Trent JM (1988) Cytogenetic and phenotypic analysis of a human colon carcinoma cell line resistant to mitoxantrone. Cancer Res 48: 1882
9. Danks MK, Yalowich JC, Beck WT (1987) Atypical multiple drug resistance in a human leukaemic cell line selected for resistance for teniposide (VM-26). Cancer Res 47: 1297
10. Egorin MJ, Hildebrand RC, Cimino EF, Bachur NR (1974) Cytofluorescence localisation of Adriamycin and daunorubicin. Cancer Res 34: 2243
11. Endicott JA, Ling V (1989) The biochemistry of P-glycoprotein-mediated multidrug resistance. Annu Rev Biochem 58: 137
12. Epstein RJ, Smith PJ (1988) Estrogen-induced potentiation of DNA damage and cytotoxicity in human breast cancer cells treated with topoisomerase-II interactive intercalative drugs. Cancer Res 48: 297
13. Estey EH, Keating MJ, McCredie KB, Bodey GP, Freirich EJ (1982) Phase II trial of dihydroxyanthracenedione in acute leukaemia. Proc Am Assoc Cancer Res 23: 113
14. Fox ME, Smith PJ (1990) Long-term inhibition of DNA synthesis and the persistence of trapped topoisomerase II complexes in determining the toxicity of the antitumor DNA intercalators mAMSA and mitoxantrone. Cancer Res 50: 5813

15. Gervasoni JE Jr, Fields SZ, Krishna S, Baker MA, Rosado M, Thurasamy K, Hindenburg AA, Taub RN (1991) Subcellular distribution of daunorubicin in P-glycoprotein-positive and -negative drug-resistant cell lines using laser-assisted confocal microscopy. Cancer Res 51: 4955
16. Ho AD, Seither E, Ma DDF, Prentice HG (1987) Mitoxantrone-induced toxicity and DNA strand breaks in leukaemic cells. Br J Haematol 65: 51
17. Kanter PM, Schwartz HS (1982) A fluorescence enhancement assay for cellular DNA damage. Mol Pharmacol 22: 145
18. Kapuscinski J, Darzynkiewicz Z, Traganos F, Melamed MR (1981) Interaction of a new antitumour agent, 1-4-dihydroxy-5,8-bis[(2-(2-hydroxyethyl)amino)-ethyl)amino]-9,10-anthracenedione, with nucleic acids. Biochem Pharmacol 30: 231
19. Krishan A, Ganapathi R (1980) Laser flow studies on the intracellular fluorescence of anthracyclines. Cancer Res 40: 3895
20. Liley DTJ, Wiggins PM, Baguley BC (1989) Localization of a nonintercalative DNA binding antitumour drug in mitochondria: relationship to multidrug resistance. Eur J Cancer Clin Oncol 25: 1287
21. Lin C-W, Shulok JR, Kirley SD, Cincotta L, Foley JW (1991) Lysosomal localisation and mechanism of uptake of Nile blue photosensitizers in tumor cells. Cancer Res 51: 2710
22. Liu LF (1989) DNA topoisomerase poisons as antitumour drugs. Annu Rev Biochem 58: 351
23. Lown JW, Hanstock CC, Bradley RD, Scraba DG (1983) Interactions of the antitumor agents mitoxantrone and bisantrene with deoxyribonucleic acids studied by electron microscopy. Mol Pharmacol 25: 178
24. Minford J, Pommier Y, Filipski J, Kohn KW, Kerrigan D, Mattern M, Michaels S, Schwartz R, Zwelling LA (1986) Isolation of intercalator-dependent protein-linked DNA strand cleavage activity from cell nuclei and identification as topoisomerase II. Biochemistry 25: 9
25. Noguchi P, Wallace R, Johnson J, Earley EM, O'Brien S, Ferrone S, Pellegrino MA, Milstien J, Needy C, Browne W, Petricciani J (1979) Characterization of WiDr: a human colon carcinoma cell line. In Vitro 15: 401
26. Roberts RA, Cress AE, Dalton WS (1989) Persistent intracellular binding of mitoxantrone in a human colon carcinoma cell line. Biochem Pharmacol 38: 4283
27. Rowe TC, Chen GL, Hsiang Y-H, Liu LF (1986) DNA damage by antitumour acridines mediated by mammalian DNA topoisomerase II. Cancer Res 46: 2021
28. Smith PJ, Makinson TA (1989) Cellular consequences of overproduction of DNA topoisomerase II in an ataxia-telangiectasia cell line. Cancer Res 49: 1118
29. Smith PJ, Morgan SA, Fox ME, Watson JV (1990) Mitoxantrone-DNA binding and the induction of topoisomerase II associated DNA damage in multi-drug resistant small cell lung cancer cells. Biochem Pharmacol 40: 2069
30. Smith PJ, Sykes HR, Fox ME, Furlong IJ (1992) Subcellular distribution of the anticancer drug mitoxantrone in human and drug-resistant murine cells analyzed by flow cytometry and confocal microscopy and its relationship to the induction of DNA damage. Cancer Res 52: 1
31. Smyth JF, Cornbleet MA, Stuart-Harris RC, Smith IE, Coleman RE, Rubens RD, McDonald M, Mouridsen HT, Rainer H, Oosterom AT van (1984) Mitoxantrone as first-line chemotherapy for advanced breast cancer: results of a European collaborative study. Semin Oncol 11: 15
32. Tewey KM, Chen GL, Nelson EM, Liu LF (1984) Intercalative antitumour drugs interfere with the breakage-reunion of mammalian DNA topoisomerase II. J Biol Chem 259: 9182
33. Wallace RE, Lindh D, Durr FE (1987) Development of resistance and characteristics of a human colon carcinoma subline resistant to mitoxantrone in vitro. Cancer Invest 5: 417
34. Watson JV (1978) A linear transform of the multi-target survival curve. Br J Radiol 51: 534
35. White JG, Amos WB, Fordham M (1987) Evaluation of confocal versus conventional imaging of biological structures by fluorescence light microscopy. J Cell Biol 105: 41
36. Yanowich S, Taub RN (1983) Differences in daunomycin retention in sensitive and resistant P388 leukemic cells as determined by digitized video fluorescence microscopy. Cancer Res 41: 67